Growth of lanthanum (III) – doped ammonium dihydrogen phosphate and tris(thiourea)zinc(II) sulfate crystals – characterization studies

Shaik Alla Nazeer [a], D. Ramasamy [b], J. Anandakumaran [a], *G. Ramasamy[a,b], ,
[a]*Department of Chemistry, Annamalai University, Annamalainagar 608 002, Tamil Nadu, India*
bDepartment of Chemistry, Government Thirumagal Mills College Gudiyattam 632602, Vellore Dt. Tamil Nadu, India

Single crystals of La(III)- doped ammonium dihydrogen phosphate (ADP) and tris(thiourea)zinc(II) sulfate (ZTS) are grown by conventional slow evaporation of aqueous solution technique. Morphological changes are observed in the doped specimen. Doping has some influence on the DRS spectra and the band gap energy is estimated by Kubelka–Munk algorithm. Incorporation of La(III)- into the crystal lattices were well confirmed by energy dispersive X-ray spectroscopy (EDS) and atomic absorption spectroscopy (AAS). The lattice parameters of the as-grown crystals were obtained by single crystal X-ray diffraction analysis. The reduction in the intensities observed in powder X-ray diffraction patterns of doped specimen and slight shifts in vibrational frequencies in fourier transform infrared spectra (FT-IR) indicate the lattice stress as a result of doping. Thermal studies reveal the purity of the material and no decomposition is observed up to the melting point. The second harmonic generations (SHG) efficiency of the host crystals are enhanced greatly in the presence of the dopant.

Keywords: A_1. Crystal growth, A_1. Doping, A_2. Growth from solution B_1.Nonlinear optical, C_1. Optical materials.

*Corresponding author

Dr. G. Ramasamy
Assistant Professor of Chemistry
Department of Chemistry
Annamalai University
Annamalainagar 608 002
Tamil Nadu, India
Cell: +91 9976756077
.

1. Introduction

Ammonium dihydrogen phosphate (ADP) crystals are widely used as the second, third and fourth harmonic generator for Nd:YAG and Nd:YLF lasers. It belongs to the tetragonal system with the space group *I-42d* [1]. These crystals are widely used for electro-optical applications such as Q-switching for Ti–sapphire and alexandrite lasers as well as for acousto optical applications [2–4]. Tris(thiourea)zinc(II) sulphate (ZTS) is a semi-organic nonlinear optical (NLO) material which finds applications in the area of laser technology, optical communication, data storage technology and optical computing because it has high resistance to laser induced damage, high nonlinearity, wide transparency, low angular sensitivity and good mechanical hardness compared to many organic NLO crystals [5–8]. It belongs to the orthorhombic system with the space group $Pca2_1$ and point group mm2. Metal ion doped materials are currently receiving a great deal of attention due to the rapid development of laser diodes [9,10]. Several foreign metallic cations existing in the parent compounds with high valance and small radii will affect the whole growth process and enhance physical properties. Their effects are related with ionic radius, electric charge, and frequency of solvent exchange [11–13]. Such additives can have a marked effect on the growth rate of the crystal faces and thus on the properties of the crystal [14]. Dopants are intentionally incorporated into the crystal structure in order to optimize the physical properties and generally lead to the generation of a charge transfer process.

Recently, we have investigated the effect of doping organic additives [15–17], Mn(II) [18], Ce(IV) [19], Cs(I) [20], Al(III), Sb(III) [21] and solvent [22] on ZTS crystals. We have investigated the effect of KCl doping on ADP specimens in detail and the studies reveal that the dopant KCl predominantly occupies the interstitial positions of ADP crystal [23,24]. The effect of metal doping on the physical and NLO properties of potassium hydrogen phthalate (KHP) crystals are studied in detail [25-28]. The effect of s, p, d and f block elements on the structure and properties of ADP [28] and KDP crystals [30,31] are dentally discussed. Effect of doping cations Li(I), Ca(II), Ce(IV) and V(V) on the properties and crystalline perfection of KDP crystals also investigated [32]. We have also investigated the influence of Ce(III)-doping [33] and organic complexing agent [34] on ADP crystals. In the present investigation, the effect of La(III)-doping on ADP and ZTS crystals has been studied using FT-IR, XRD, SEM, EDS, UV–Vis, thermal and Kurtz powder SHG measurements.

2. Experimental

2.1. Synthesis and crystal growth

ADP (E. Merck) was purified by repeated recrystallization. The ZTS was synthesized [35] in the stoichiometric ratio of 1:3 for zincsulphate heptahydrate (EM) and thiourea (SQ). To avoid decomposition, low temperature (<70˚ C) was maintained during the preparation of the solution in deionized water.

$$ZnSO_4 \cdot 7H_2O + 3(CS(NH_2)_2) \rightarrow Zn(CS(NH_2)_2)_3SO_4$$

After successive recrystallization processes, crystals were grown by slow evaporation solution growth technique (pH = 6.2) as detailed in our previous studies [17-20]. Doping of lanthanum (5 mol%) in the form of lanthanum(III) chloride (Aldrich) was used as such in the aqueous growth medium. The crystallization took place within 10–15 days and the high quality transparent crystals were harvested from the aqueous growth medium. Best quality and highly transparent seed crystals are used in the preparation of bulk crystals. Photographs of the as- grown crystals obtained are shown in Fig. 1.

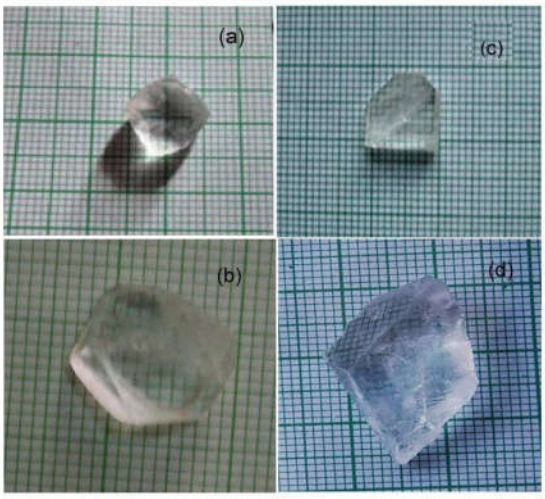

Fig.-1:-Photograph of (a) pure ADP (b) ADP:La (c) pure ZTS (d) ZTS:La crystals

2.2. Characterization techniques

The FT-IR spectra were recorded by using an AVATAR 330 FT-IR instrument by KBr pellet technique in the range 500-4000 cm^{-1}. Bruker AXS (Kappa Apex II) X-ray diffractometer was used for single crystal XRD studies. The powder X-ray diffraction was

performed by using Philips Xpert Pro Triple-axis X-ray diffractometer at room temperature at a wavelength of 1.540 Å with a step size of 0.008º. The samples were examined with CuKα radiation in the 2θ range from 10 to 60º. The XRD data were analyzed by the Rietveld method with RIETAN–2000. The surface morphologies was observed by using a JEOL JSM 5610 LV SEM with the resolution of 3.0 nm, an accelerating voltage 20 kV and maximum magnification 3,00,000 times. Energy dispersive X-ray spectroscopy (EDS), a chemical microanalysis technique was performed in conjunction with SEM. AAS was recorded using VARIAN Model SPECTRAA 220 spectrometer in acetone – air flame. This technique is used to quantify the concentration of the dopant present in ADP and ZTS crystals using a graphite line as internal standard. UV-Vis- DRS spectra were recorded using Varian Cary 5E UV-Vis-NIR spectrophotometer. TG–DTA studies were carried out on a SDT Q600 Thermal analyzer TA Instrument between 25–600 ˚C in nitrogen atmosphere, at a heating rate of 10 ˚C min^{-1}. 0.5 g of sample taken in an Al_2O_3 crucible is placed on top of a thermocouple resting on a balance, and the system is sealed into a chamber and heated with a constant heating rate. The second harmonic generation (SHG) test on the crystals was performed by Kurtz powder SHG method. An Nd:YAG laser with modulated radiation of 1064 nm was used as the optical source with an input radiation of 2.5 mJ/ pulse and the grown crystals were ground to a uniform particle size of 125 to 150 μm and then packed in a micro-capillary of uniform bore and exposed to laser radiation. The output from the sample was monochromated to collect the intensity of the 532 nm component and to eliminate the fundamental. Microcrystalline KDP was used as a reference material.

3. Results and discussion

3.1 FT-IR analysis

The FT-IR spectra of pure and doped crystals reveal that the characteristic vibrational patterns of pure and doped ADP crystals are very close to each other (Fig.2[a & b]). Small shifts in some of the characteristic vibrational frequencies are observed (Table. 1). It could be due to lattice strain as a result of La(III)- doping.

A close observation of FT-IR spectra (Fig. 2[c & d]) of pure ZTS and doped specimens reveal that the doping results in slight shifts in some of the characteristic vibrational frequencies. It could be due to lattice strain developed as a result of doping. An absorption band in the region 2750–3400cm^{-1} corresponds to the symmetric and asymmetric stretching frequencies of NH_2 group of zinc (II) coordinated thiourea. The absorption band observed at ~1620 cm^{-1} in the spectra of pure and doped specimen corresponds to that of

thiourea (~1625 cm^{-1}) [36] of about the same frequency and it can be assigned to NH_2 bending vibration. The CN stretching frequencies of thiourea (1089 and 1472 cm^{-1}) are shifted to higher frequencies for pure and La(III)- doped ZTS crystals (~1090 and ~1500 cm^{-1}). The CS stretching frequencies (1417 and 740cm^{-1}) [37] are shifted to lower frequencies (~1394 and ~706 cm^{-1}) for pure and doped samples. These observations suggest that metal coordinate with thiourea through sulfur atom.

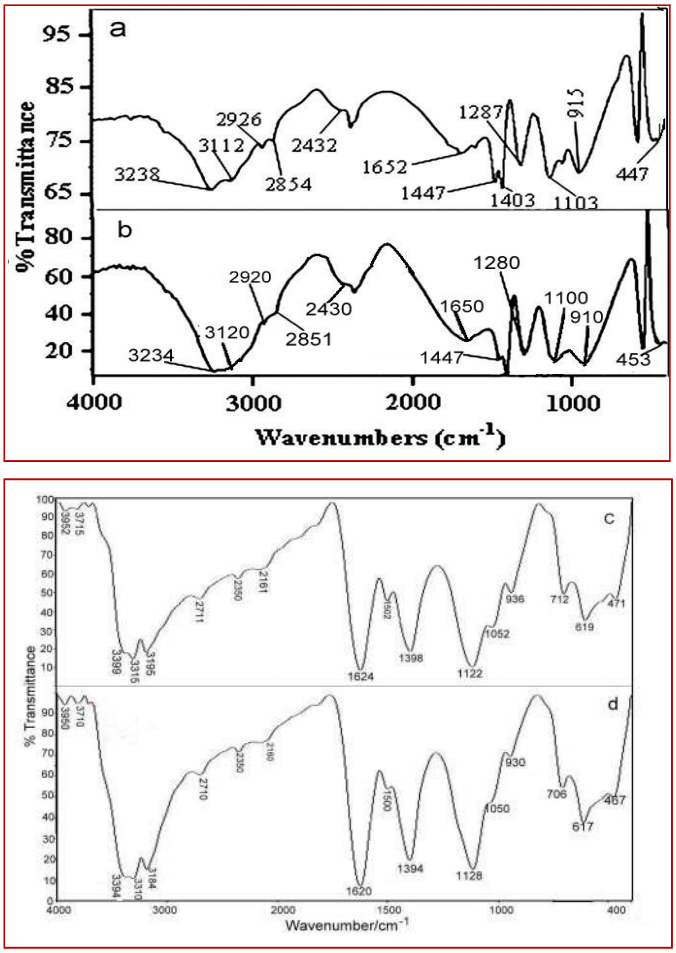

Fig.-2:- FT-IR spectrum of (a) pure ADP (b) ADP:La (c) pure ZTS and (d) ZTS:La

Table 1
Frequencies of fundamental vibrations of pure ADP, ADP:La, pure ZTS and ZTS:La samples/cm^{-1}

Assignment of vibrations	ADP	ADP:La	Assignment of vibrations	ZTS	ZTS:La
PO_4 stretching	1103 915	1100 910	$\nu_{as}(NH_2)$	3399	3394
PO_4 bending	447 544	453 546	$\nu_s(NH_2)$	3195	3184
			$\delta(NH_2)$	1624	1620
$-NH_4$ stretching	1403	1407	ν_s(C-N)	1122	1128
			ν(N-C-N)	1502	1500
–OH bending	1287	1280	ν_{as}(C=S)	1398	1394
			ν_s(C=S)	712	706
N–H···O stretching	3238	3234 3120	ν_{as}(N-C-S)	619	617
			δ_{as}(N-C-N)	471	467

3.2 XRD analysis

The powder XRD patterns of La(III)-doped samples are compared with that of undoped one (Fig. 3). No new peaks or phases were observed by doping with inner transition metal lanthanum. However, a drastic reduction in intensity is observed as a result of doping. The most prominent peaks with maximum intensity of the XRD patterns of pure and doped specimens are quite different. The observations could be attributed to strains in the lattice.

The cell parameters are determined from the single crystal X-ray diffraction analysis and the values of pure and doped crystals are given in the Table 2. The ionic radius of the dopant La(III) (117 pm) is very small compared with that of NH_4^{1+} (151 pm)[29]. Hence, it is reasonable to believe that the dopant can enter into the ADP crystalline matrix occupying predominantly substitutional positions without causing much distortion and the cell volume is expected to be reduced due to the small size of a substituted rare earth ion. In the present investigation, the dependence of the lattice parameter 'c' and the volume on [La(III)] clearly reveal that the crystal undergoes non-uniform strain. The reverse trend is noticed in ZTS crystals but to a lesser extent (Fig. 3). It could be due to the small ionic radius of Zn^{2+} (88 pm) in comparison with that of La(III) (117 pm)[30]. This type of behaviour (the unit cell volume

of the doped materials not varying regularly with the ionic radius of the dopant) has been explained by the electron-doping effect counteracting the steric effect[38].

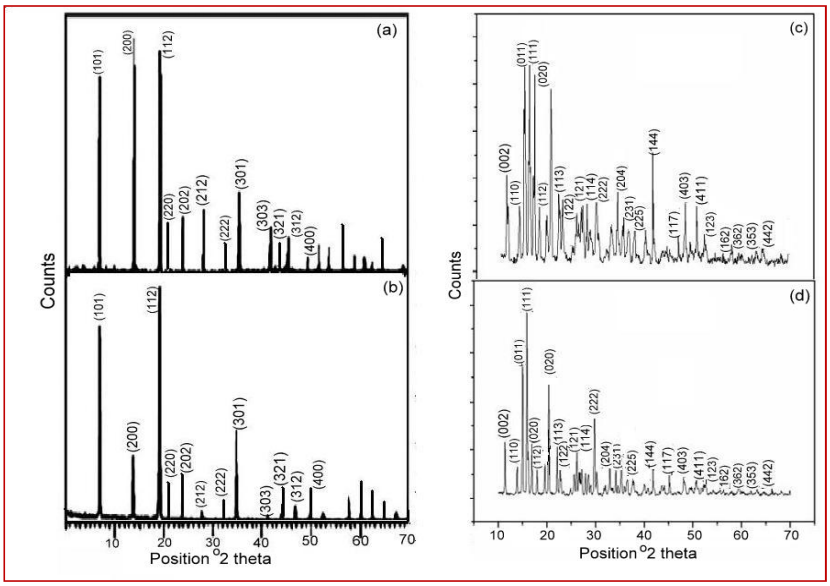

Fig.-3:- Powder XRD patterns of (a) pure ADP (b) ADP:La (c) pure ZTS and (d) ZTS:La.

Table 2

Cell parameter of as grown crystals

System	a (Å)	b (Å)	c (Å)	V (Å^3)	⍰=β=γ
ADP	7.510	7.510	7.564	425	90˚
ADP:La	7.536	7.536	7.570	429	90˚
ZTS	11.212	7.722	15.638	1350	90˚
ZTS:La	11.230	7.799	15.591	1361	90˚

3.3. Diffuse reflectance spectral analysis

A close observation of DRS reveals that there are significant changes in the DRS as a result of doping. In both ADP and ZTS crystals the doping of La(III) drastically increases the reflectance (lowering the absorption) 40% to 60% in the case doped ADP crystals and 30% to 45% in the case doped ZTS crystals (Fig. 4) and hence La(III) is a useful dopant like Ce(IV) [19]. It has been reported that the reflectance of KCl was found to vary with the particle size

[39]. The concentration of absorbing species can be determined using the Kubelka-Munk equation [40], correlating reflectance and concentration,

$$F(R) = (1\text{-}R)^2/2R = \alpha/s = Ac/s \quad \ldots\ldots(1)$$

Where *F(R)* is Kubelka-Munk function, R is the reflectance of the crystal and S is scattering coefficient, A is the absorbance and c is concentration of the absorbing species. The direct and indirect band gap energy obtained from the intercept of the resulting straight line with the energy axis at $[F(R)hv]^2 = 0$ and $[F(R)hv]^{1/2} = 0$ are deduced as 5.35 eV & 5.5 eV for ADP:La and 5.37 eV & 5.7 eV for ZTS:La (Fig. 4).

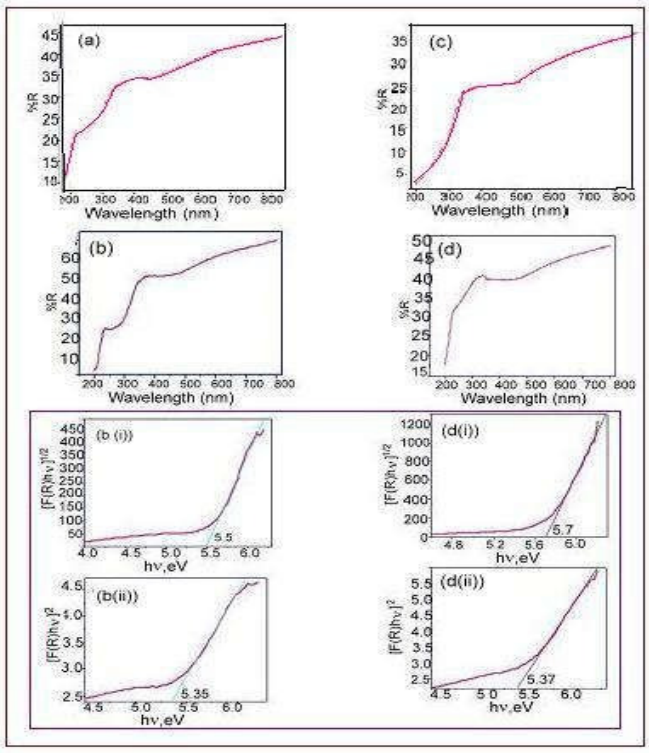

Fig.-4:- DRS specra of (a) pure ADP (b) ADP:La (c) Pure ZTS (d) ZTS:La Tauc plot of (b(i)) direct band gap of ADP:La (b(ii)) Indirect band gap of ADP:La (d(i)) direct band gap of ZTS:La (d(ii)) indirect band gap of ZTS:La

3.4 SEM

The effect of the influence of dopant on the surface morphology of ADP crystal faces reveals structure defect centers as seen in SEM images (Fig. 5). A plate like morphology with a layered structure in exhibited in pure ADP crystal (Fig. 5(a)). The incorporation of

lanthanum in the ADP crystal matrix results in cluster of scatter centers and voids than those of the undoped specimen. The flower like morphology of is observed in doped specimen of ZTS crystal. Pure ZTS contains small defect centers in the plate surface, incorporation of La(III) increases the surface roughness (Fig. 5(d)).

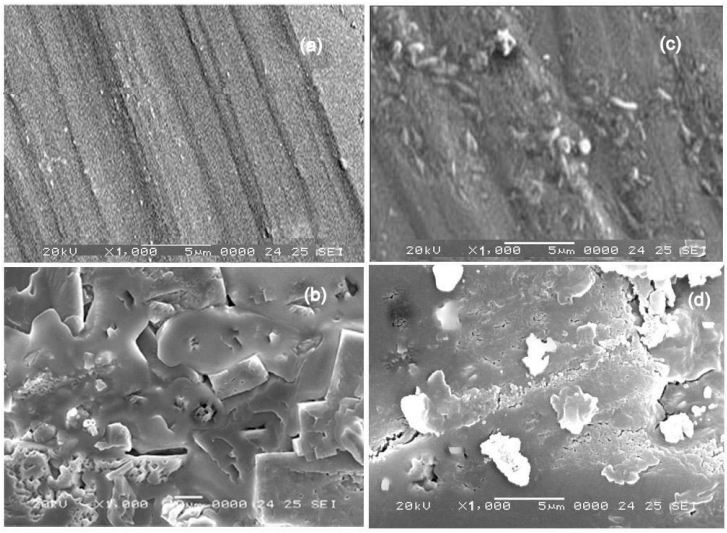

Fig.-5:- SEM images of (a) pure ADP (b) ADP:La (c) pure ZTS (d) ZTS:La crystals

3.5 EDS and AAS analysis

The incorporation of La(III) into the crystalline matrix was confirmed by EDS performed on ADP and ZTS (Fig. 6). It appears that the accommodating capability of the host crystal is limited and only a small quantity is incorporated into the ADP and ZTS crystalline matrix. EDS spectra reveal that the accommodating capability of ZTS is much better than ADP as shown in (Fig.6).

The amounts of dopant in ADP:La and ZTS:La specimens are estimated using AAS and the foreign metal ion entering into the ADP/ZTS crystal matrix is much smaller but significant. Further, the final dopant concentration within the host lattice is not proportional to the prevailing concentration of dopant in the solution at the time of the crystallization process, since the host crystal can accommodate the dopant only to a limited extent. The AAS data reveal that the La(III) ion concentration in ADP and ZTS crystalline matrix are 7.5 ppm and 11.3 ppm respectively (where as the Zn(II) ion concentration in doped ZTS is 512 ppm). High incorporation of the dopant in the case of lanthanide doping in KHP compared to the transition metal, Ru(III) (1.45 ppm of Ru(III)) [19] is expected, since the charge density in the case of lanthanides is high because of the small size (lanthanide contraction) and high valency.

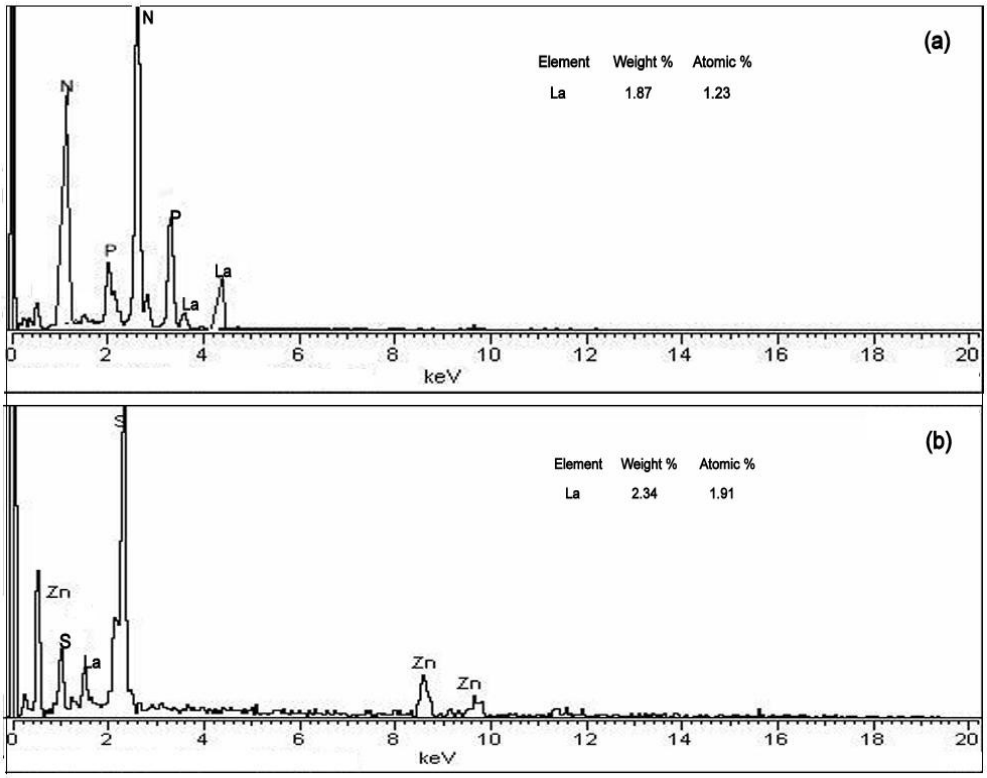

Fig.-6:- EDS spectra of (a) ADP:La (b) ZTS:La

3.6 Thermal studies

TG/DTA thermogram reveals the purity of the material. The thermogram curve shows a gradual mass loss and residual mass obtained at 1000 ˚C is only 15% (Fig. 7(a) & (b)). An endothermic peak is obtained in the DTA analysis for ADP:La at a higher temperature (200 ˚C) than the pure ADP crystals (191 ˚C). Melting point of the material was confirmed by using Sigma instruments melting point apparatus (200 ˚C). the investigation shows that there is no physically absorbed water in molecular structure of crystals grown from the solution.

The simultaneous TG-DTA curves in nitrogen for ZTS and ZTS:La systems at a heating rate of 20 ˚C/min are given in the Fig. 7(c) and (d). The absence of water of crystallization in the molecular structure is indicated by the absence of weight loss around 100 ˚C. Melting point of the sample is slightly lower in the case of La(III)- doped ZTS (Fig. 7(d)). A very good thermal stability of the material is observed up to ~ 235 ˚C and the thermal behavior is not very much altered in the presence of the dopant. The sharp endothermic peak at 235 ˚C is may be due to melting point. TG curve shows a gradual mass loss and residual mass obtained at 1000 ˚C is ~ 20 %. The sharpness of the peak shows the

good degree of crystallinity of the material. No decomposition up to the melting point ensures the stability of the material for application in laser, where the crystals are required to withstand high temperatures.

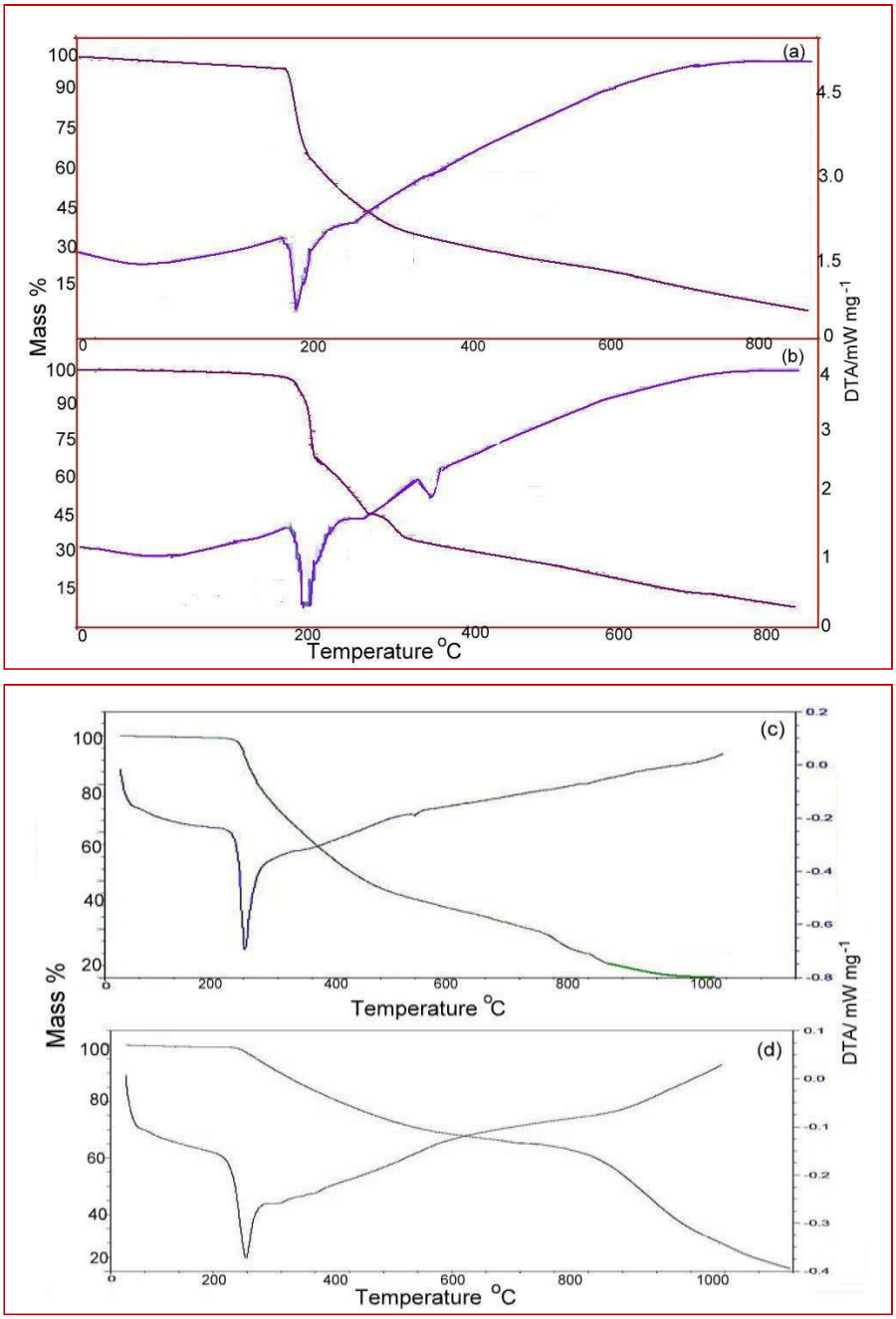

Fig.-7:- TG/DTA curves of (a) pure ADP (b) ADP:La (c) pure ZTS (d) ZTS:La

3.7 SHG efficiency

In order to confirm the influence of doping on the nonlinear optical properties (NLO) of the as-grown crystals, these were subjected to SHG test. SHG teat on the materials was

performed by Kurtz powder SHG method [40]. Input radiation used is 2.5 mJ/pulse. The output SHG intensities of La(III) doped ADP and ZTS specimens give relative NLO efficiencies of the measured specimens. The doubling of frequency was confirmed by the green color of the output radiation whose characteristic wavelength is 532 nm. Green color output indicates that the doped material exhibits second order NLO effect. The depressed SHG efficiency is quite likely due to the disturbance of charge transfer. The efficient SHG demands specific molecular alignment of the crystal to be achieved facilitating nonlinearity in the presences of a dopant. It has been reported that the SHG can be greatly enhanced by attaining the molecular alignment through inclusion complexation [41]. Recently, we have reported that enhancement in crystalline perfection could lead to improvement in SHG efficiency [23]. Incorporation of La(III) in to ADP and ZTS crystalline matrix enhances the SHG efficiency (Table . 3) and hence La(III) is a useful dopant. The efficient SHG demands specific molecular alignment of the crystal facilitating nonlinearity in the presence of dopant or it may be due to the improvement in the crystalline perfection of ADP/ZTS crystals by low level La(III)- doping. The effect of various dopants on the SHG efficiency of the ADP and ZTS crystal has been listed in Table. 4.

Table 3

SHG Outputs (Input 2.5 mV/pulse)

System	$I_{2\omega}$ /mV
KDP	38
ADP	29
ADP:La	37
ZTS	17
ZTS:La	23

Table 4
SHG outputs of ZTS and ADP with various dopants.

Doped ZTS crystals			Doped ADP crystals		
System	$I_{2\omega}$ /mV	**Ref**	**System**	$I_{2\omega}$ /mV	**Ref**
ZTS doped with La(III)	1.35 times higher than ZTS	Present work	ADP doped with La(III)	1.3 times higher than ZTS	Present work
ZTS doped with Cs(I)	1.2 times higher than ZTS	[20]	ADP doped with Ce(IV)	Enhances SHG efficiency	[32]
ZTS doped with EDTA	1.8 times higher than ZTS	[16]	ADP doped with KCl	2 times higher than ADP	[22]
ZTS doped with Benzene	1.5 times higher than ZTS	[16]	ADP doped with oxalic acid	Slightly greater than ADP	[22]
ZTS doped with 1,10-Phenanthroline	Half the value of ZTS	[15]	ADP doped with Cs(I)	1.2 times higher than ADP	[28]
ZTS doped with Mn(II)	2.1 times higher than ZTS	[18]	ADP doped with Sb(III)	Similar to ADP	[28]
ZTS doped with Ce(IV)	1.6 times higher than ZTS	[19]	ADP doped with Ce(IV)	1.1 times higher than ADP	[28]
ZTS doped with KI	1.2 times higher than KDP	[42]	ADP doped with Pd(II)	1.1 times higher than ADP	[28]
ZTS doped with KCl	1.2 times higher than KDP	[43]	ADP doped with L-asparagine	Similar to ADP	[49]
ZTS doped with LiBr	Green light emission	[44]	ADP doped with Hippuric acid	1.5 times higher than ADP	[50]
ZTS doped with Na(I)	Slightly greater than ZTS	[45]	ADP doped with DL- malic acid	1.5 times higher than ADP	[51]
ZTS doped with urea	2 times higher than ZTS	[46]	ADP doped with ammonium acetate	Enhances the SHG efficiency	[52]
ZTS doped with L-lysine	similar to ZTS	[47]	ADP doped with L-tartaric acid	Slightly enhances the SHG efficieny	[53]
ZTS doped with glycine	4.1times higher than ZTS	[48]	ADP doped with L-alanine	Higher than ADP	[54]
ZTS doped with Al(III)	1.09 times higher than ZTS	[21]	ADP doped with thiourea	1.1 time higher than ADP	[55]
ZTS doped with Sb(III)	1.25 times higher than ZTS	[21]	ADP doped with ZnS	3.7 times higher than ADP	[56]

4. Conclusion

The influence of La(III) doping on the ADP and ZTS crystal have been studied. The reduction in the intensities observed in the powder XRD pattern and slight shifts in vibrational frequencies in FT-IR indicates minor structural variations in the doped materials. Morphological changes in the doped specimen are observed in the SEM micrographs. The studies indicate that the crystal undergoes lattice stress as a result of doping. Energy dispersive X-ray spectrum reveals the incorporation of La(III)- into the crystalline matrix of ADP/ZTS crystals. AAS studies also confirm quantitatively, the above results. From EDS and AAS studies the incorporation of La(III)- is comparatively high in the case of doped ZTS crystals. The thermal analysis reveals purity of the material; stability of material is slightly higher in the case of doped ADP crystals and slightly lowered in the case of doped ZTS crystals. Diffused reflection spectroscopy reveals the percentage reflection increases in the doped specimen compared to that of pure ADP/ZTS. Enhancement in SHG efficiency is observed in both ADP/ZTS crystals as a result of La(III)- doping.

References

[1] H. Mcmurdie, M. Morris, E. Evans, B. Peretzkin, W. Wong-Ng, Y. Zhang, Powder Diffraction 1 (1986) 335–345.

[2] N. Zaitseva, L. Carman, Progress in Crystal Growth and Characterization of Materials 43 (2001) 1–118.

[3] S.M Klimentov, S.V. Garnov, A.S. Epifanov, A.A. Manenkov, Proceedings of SPIE 2145 (1994) 342–354.

[4] R. Ramirez, J.A. Gonzala, Solid State Communications 75 (1990) 482–491.

[5] S.S. Gupta, C.F. Desai, Cryst. Res. Technol. 34 (1999) 1329–1332.

[6] U.B. Ramabadran, D.E. Zelmon, G.C. Kennedy, Appl. Phys. Lett. 60 (1992) 2589–2591.

[7] P.U. Sastry, Solid State Commun. 109 (1999) 595–598.

[8] V. Venkataramanan, G. Dhanaraj, V.K. Wadhawan, J.N. Sherwood, H.L. Bhat, J. Cryst. Growth 154 (1995) 92–97.

[9] X. Long, G. Wang, T.P.J. Han, J. Cryst. Growth 249 (2003) 191–194.

[10] J. Ramajothi, S. Dhanuskodi, Cryst. Res. Technol. 38 (2003) 986–991.

[11] T. Ohachi, M. Hamanada, H. Konda, D. Hayashi, I. Taniguchi, T. Hashimoto, Y.J. Kotani, J. Cryst. Growth 99 (1990) 72–76.

[12] X.Q. Wang, D. Xu, M.K. Lu, D.R. Yuan, J. Huang, S.G. Li, G.W. Lu, H.Q. Sun, S.Y. Guo, G.H. Zhang, X.L. Duan, H.Y. Liu, W.L. Liu, J. Cryst. Growth 247 (2003) 432–

437.

[13] R. Uthrakumar, C. Vesta, C. Justin Raj, S. Dinakaran, R. Christhu Dhas, S. Jerome Das, Cryst. Res. Technol. 43 (2008) 428–432.

[14] P.M. Ushasree, R. Jayavel, P. Ramasamy, Materials Chemistry and Physics 61 (1999) 270–274.

[15] S.P. Meenakshisundaram, S. Parthiban, R. Kalavathy, G. Madhurambal, G. Bhagavannarayana, S.C. Mojumdar, J. Therm. Anal. Calorim. 100 (2010) 831–837.

[16] S. Meenakshisundaram, S. Parthiban, N. Sarathi, R. Kalavathy, G. Bhagavannarayana, J. Cryst. Growth 293 (2006) 376–381.

[17] G. Bhagavannarayana, S. Parthiban, Subbiah Meenakshisundaram, J. Appl. Crystallogr. 39 (2006) 784–790.

[18] G. Bhagavannarayana, S.K. Kushwaha, S. Parthiban, S. Meenakshisundaram, J. Cryst. Growth 311 (2009) 960–965.

[19] L. Kasthuri, G. Bhagavannarayana, S. Parthiban, G. Ramasamy, K. Muthu, Subbiah Meenakshisundaram, Cryst. Eng. Commun. 12 (2010) 493–499.

[20] K. Muthu, SP. Meenakshisundaram, J. Chem. Phys. Solid. 73 (2012) 1146-1150.

[21] K. Meena, G. Ramasamy, M. Rajasekar, K. Muthu, S. P. Meenakshisundaram, Optik. 125 (2014) 4876-4880.

[22] S. Meenakshisundaram, S. Parthiban, G. Bhagavannarayana, G. Madhurambal, S.C. Mojumdar, J. Therm. Anal. Calorim. 96 (2009) 125–129.

[23] G. Bhagavannarayana, S. Parthiban, S. Meenakshisundaram, Crystal Growth and Design 8 (2008) 446–451.

[24] S. Meenakshisundaram, S. Parthiban, G. Madhurambal, S.C. Mojumdar, J. Therm. Anal. Calorim. 96 (2009) 77–80.

[25] S. Parthiban, S. Murali, G. Madhurambal, S. P. Meenakshisundaram, S.C. Mojumdar, J.Therm. Anal. Calorim. 100 (2010) 751–756.

[26] G. Ramasamy, S. Parthiban, S.P. Meenakshisundaram, S.C. Mojumdar, J.Therm. Anal. Calorim. 100 (2010) 861–865.

[27] K. Muthu, G. Bhagavannarayana, C. Chandrasekaran, S. Parthiban, S.P. Meenakshisundaram, S.C. Mojumdar, J. Therm. Anal. Calorim, 100 (2010) 793–799.

[28] G. Bhagavannarayana, S. Parthiban, C. Chandrasekaran, S. Meenakshisundaram, Cryst. Engg. Comm. 11 (2009) 1635–1641.

[29] M. Amutha, G. Ramasamy, S. P. Meenakshisindaram, S. C. Mojumdar, J.Therm. Anal.

Calorim. 104 (2011) 949–954.

[30] G. Ramasamy, G. Bhagavannarayana, S. P. Meenakshisundaram, Cryst. Engg. Comm. 14 (2012) 3813–3819.

[31] G. Ramasamy, S. P. Meenakshisundarm, S. C. Mojumdar, J.Therm. Anal. Calorim. 112(2013) 1121–1125.

[32] G. Ramasamy, G. Bhagavannarayana, S. P. Meenakshisundaram, Indian J. Pure & Appl. Phys. 52 (2014) 255-261.

[33] K. Vanchinathan, K. Muthu, G. Bhagavannarayana, S. P. Meenakshisundaram, J. Crystal Growth 354 (2012) 57-61.

[34] SP. Meenakshisundaram, S. Parthiban, G. Madhurambal, R. Dhanasekaran, S.C. Mojumdar, J. Therm. Anal. Calorim. 94 (2008) 15–20.

[35] P.M. Ushasree, R. Muralidharan, R. Jayavel, P. Ramasamy, J. Cryst. Growth 210 (2000) 741–745.

[36] C. Krishnan, P. Selvarajan, T.H. Freeda, J. Cryst. Growth 311 (2008) 141–146.

[37] J. Ramajothi, S. Dhanuskodi, K. Nagarajan, Cryst. Res. Technol. 39 (2004) 414–420.

[38] Q. Zhang, G. H. Rao, Y. G. Xiao, H. Z. Dong, Y. Liu, Y. Zhang, J. K. Liang, Phys. B. 381 (2006) 233-238.

[39] M. P. Fuller, P. R. Griffiths, Anal. Chem. 50 (1978) 1906-1910.

[40] P. Kubelka, J. Opt. Soc. Am 38 (1948) 448-457.

[41] M. Rak, N. N. Eremin, T. A. Eremina, V. A. Kuznetsov, T. M. Okhrimenko, N. G. Furmanova, J. Crystal Growth. 273 (2005) 577-585.

[42] C. Krishnan, P. Selvarajan, T.H. Freeda, J. Cryst. Growth 311 (2008) 141–146.

[43] C. Krishnan, P. Selvarajan, T.H. Freeda, Mater. Lett. 62 (2008) 4414–4416.

[44] C. Krishnan, P. Selvarajan, T.H. Freeda, Mater. Manuf. Processes 23 (2008) 800–804.

[45] C. Krishnan, P. Selvarajan, S. Pari, Curr. Appl. Phys. 10 (2010) 664–669.

[46] G. Bhagavannarayana, S.K. Kushwaha, J. Appl. Cryst. 43 (2010) 154–162.

[47] J. Thomas Joseph Prakash, M. Lawrence, Int. J. Comput. Appl. 2 (2010) 36–39.

[48] N.R. Dhumane, S.S. Hussaini, V.G. Dongre, M.D. Shirsat, Opt. Mater. 31 (2008) 328–332.

[49] P. Rajesh, P. Ramasamy, Phys. B. 405 (2010) 1287-1293.

[50] A. Kumaresh, R. Arunkumar, Sectrochim. Acta A121 (2014) 346-349.

[51] P. Rajesh, P. Ramasamy, J. Crystal Growth. 311 (2009) 3491-3497.

[52] P. Rajesh, K. Boopathi, P. Ramasamy, J. Crystal Growth. 318 (2011) 751-756.

[53] M. Hasmuddin, P. Singh, M. Shkir, M. M. Abdullah, N. Vijayan, V. Ganesh,

M. A. Wahab, Matter. Chem. Phys. 144 (2014) 293-300.

[54] R. N. Shaikh, S. R. Mitkar, M. Anis, M. D. Shirsad, S. S. Hussaini, Int. J. Chemtech. Res. 6 (2014) 1617-1620.

[55] A. Jayarama, S. M. Dhramaprakash, Indian J. Pure App. Phys. 43 (2005) 859-862.

[56] J. Anitha Hudson, C. K. Mahadevan, C. M. Padma, Int. J. Res. Engg. Technol. 2 (2013) 674-683.